THE JOURNAL OF PHYSICAL CHEMISTRY B

Article

pubs.acs.org/JPCB

Theoretical Study of Salt Effects on the Diels–Alder Reaction of Cyclopentadiene with Methyl Vinyl Ketone Using RISM-SCF Theory

Norio Yoshida,*[,†] Hidetsugu Tanaka,[‡] and Fumio Hirata*[,§]

[†]Department of Chemistry, Graduate School of Sciences, Kyushu University, 6-10-1 Hakozaki, Higashi-ku, Fukuoka 812-8581, Japan

[‡]Advancing Analysis Laboratory, Mitsui Chemicals, Inc., 580-32 Nagaura, Sodegaura Chiba 299-0265, Japan

[§]College of Life Sciences, Ritsumeikan University, Kusatsu, Shiga 525-8577, Japan

ABSTRACT: Salt effects on the Diels–Alder reaction of cyclopentadiene with methyl vinyl ketone are investigated using reference interaction site model self-consistent field (RISM-SCF) theory. The rate of the reaction is accelerated by adding LiCl to the water solvent. The structures of four transition states, *endo*-cis, *endo*-trans, *exo*-cis, *exo*-trans, were found by geometry optimization of the cyclopentadiene and methyl vinyl ketone complexes. The *endo*-trans structure shows the lowest energy in both water and LiCl solution. The activation barrier of the reaction in LiCl solution is lower than that in water, and the difference is in good agreement with that from experiments. The decrease in the activation barrier arises from destabilization of the reactant species. The salt effect of LiCl makes all species concerning the reaction unstable by the hydrophobic effect; however, the increased hydrophobic effect in the TS complexes is suppressed by making the hydrogen bond, which is stronger compared with the reactant methyl vinyl ketone.

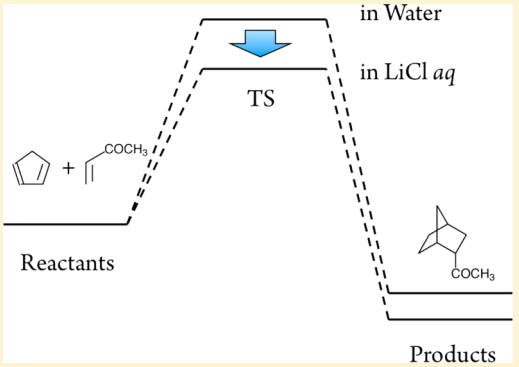

INTRODUCTION

The Diels–Alder reaction has been studied a lot both experimentally and theoretically as it is one of the most important and valuable reactions to form carbon–carbon bonds. In particular, solvent effects on the reaction are most noteworthy because they play a key role in determining the rate of the reaction.[1] It has been known that the rate of the reaction is accelerated dramatically in aqueous solution compared with that in organic solvents. A number of computational and theoretical studies have been devoted to clarify the mechanism of acceleration by water.[2−13] These studies have concluded that the primary factor responsible for the acceleration is the reduction in hydrophobic surface area as the cycloaddition proceeds and enhanced hydrogen bonding between water and reactant molecules in the transition state (TS).[1,7,8,14]

In the Diels–Alder reaction between cyclopentadiene (CP) and methyl vinyl ketone (MVK), the rate of the reaction is accelerated 2.5 times by adding LiCl to an aqueous solution at room temperature (see Scheme 1). It is believed that the electrolytes enhance the hydrophobic interactions between the two reactants. However, this is only conjecture and may be difficult to prove just from experiments. Therefore, the theoretical approach may be a useful way to prove the conjecture.

Scheme 1. Schematic Description of the Diels–Alder Reaction between CP and MVK

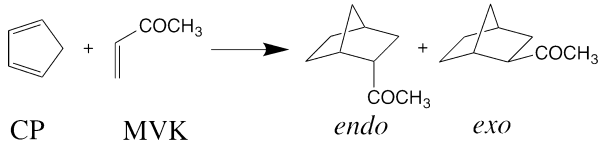

To do this, two important solvent effects, the hydrophobic and salt effects, should be treated properly. Continuum solvent models such as the polarizable continuum model (PCM) and the generalized Born (GB) model are inadequate in this respect because they disregard the molecularity of the solvent, and thus, they cannot handle the hydrophobicity.[15] On the other hand, molecular simulations such as Monte Carlo (MC) and molecular dynamics (MD) have difficulty in treating the salt effect for the reaction Gibbs energy because the convergence of the sampling configuration space of ions in dilute salt concentrations is extremely slow.[16]

The reference interaction site model self-consistent field (RISM-SCF) theory is a promising way to tackle the problem.[17,18] It can handle both the hydrophobicity and salt effects from first-principles without making any unwarranted assumptions concerning the solvent effect. The solvent effects on the solute electronic structure are considered by means of the RISM integral equation theory, which is a statistical mechanics theory of molecular liquids.[19−24] The RISM theory has been successfully applied to investigate various chemical and biological phenomena.[25−28] Harano et al. employed the RISM-SCF method to investigate the solvent effect in a Diels–Alder reaction in ambient and supercritical water.[4] Most

Received: September 12, 2013
Revised: October 20, 2013
Published: October 21, 2013

recently, Hayaki et al. have applied the extended version of RISM-SCF method, referred to as the RISM-SCF-SEDD method,[29] to Diels–Alder reactions in ionic liquids.[13] The RISM-SCF method has been successfully applied to reveal the mechanism of stereoselectivity of the reaction. Imai et al. applied the RISM theory to the salt effect on the stability of the peptide conformation to clarify the physical origin of the Hofmeister series.[30] Some authors applied the RISM theory to investigate ion binding by human lysozyme in LiCl, NaCl, KCl, and $CaCl_2$ aqueous solutions.[31−33] In these papers, the selective ion binding by a variety of mutants of human lysozyme was reproduced in good agreement with corresponding experiments. In their calculations, the mean activity coefficients of electrolyte solutions, the most fundamental physicochemical properties characterizing electrolyte solutions, were reproduced reasonably well. Those applications demonstrate unequivocally that the RISM theory can be applied to investigate the salt effect on chemical and physical phenomena in solution.

In the present study, we employ the RISM-SCF theory to investigate the Diels–Alder reaction in both water and an aqueous solution of LiCl. The stable structures of CP and MVK were optimized in both water and an aqueous LiCl solution using the analytical energy gradient of the RISM-SCF formula.[34] A stationary point search was also performed to find the TS structure. Four types of TS structures, *endo*-cis, *endo*-trans, *exo*-cis, and *exo*-trans, were found and compared in terms of the Gibbs energy difference between reactants. A component analysis of the Gibbs energy change was performed to clarify the origin of salt effects on the reaction. The solvation structures of all TSs were also considered to probe the salt effects.

COMPUTATIONAL DETAILS

Here, we show some equations that are conceptually important and necessary to discuss the results. The details of the theory are available in some of our previous articles.[17,18,24,34] The total Gibbs energy (G) of the solute in the solvent is defined as a sum of the solute electronic energy (E_0), the solvation free energy (G_{solv}), and the kinetic free energy (G_{kin})

$$G = E_0 + G_{solv} + G_{kin} \tag{1}$$

The terms have the following meanings

$$E_0 = \langle \Psi_0^{solv} | \hat{H}_0 | \Psi_0^{solv} \rangle \tag{2}$$

where $\hat{H}_0$ is the Hamiltonian of the isolated molecules and Ψ_0^{solv} is the wave function of the solute molecule in isolated systems keeping the geometry optimized in solution. The solvation free energy is defined by the sum of the electronic distortion energy (E_{dist}) and the excess chemical potential ($\Delta\mu$). For the excess chemical potential, we adopted the expression derived from the closure relation proposed by Kovalenko and Hirata[35,36]

$$\Delta\mu = 4\pi \sum_{\nu \in \text{solvent species}} \frac{\rho_\nu}{\beta} \sum_{\alpha \in \text{solute site}} \sum_{\gamma \in \text{solvent site on } \nu} \times \int \left[\frac{1}{2} h_{\alpha\gamma}^2(r)\Theta(-h_{\alpha\gamma}) - c_{\alpha\gamma}(r) - \frac{1}{2} h_{\alpha\gamma}(r) c_{\alpha\gamma}(r) \right] r^2 \, dr \tag{3}$$

where $c_{\alpha\gamma}$ and $h_{\alpha\gamma}$ are the direct and total correlation functions between site α on the solute and γ on the solvent, respectively. The symbol $h_{\alpha\gamma}$ is related to the radial distribution function (RDF) by $g_{\alpha\gamma} = h_{\alpha\gamma} + 1$. The symbol Θ denotes the Heaviside step function, which puts the term $h_{\alpha\gamma}^2$ into effect in the regions of density depletion only, and $\beta = (1/k_B T)$ is the inverse of the product of the Boltzmann factor k_B and the thermodynamic temperature T. The electronic distortion energy can be defined as

$$E_{dist} = E_{solute} - E_0 = \langle \Psi^{solv} | \hat{H}_0 | \Psi^{solv} \rangle - \langle \Psi_0^{solv} | \hat{H}_0 | \Psi_0^{solv} \rangle \tag{4}$$

where Ψ^{solv} is the wave function of the solute molecule in solution. Therefore, the electronic distortion energy means the electronic energy change caused by the change of the electronic structure by solvation. The symbol G_{kin} denotes the kinetic free-energy term of the solute molecule, which includes the energies of translation, rotation, and vibration.

The solvation free energy G_{solv} can be decomposed into the solute–solvent interaction energy $\Delta\varepsilon_{uv}$, the solvent reorganization energy $\Delta\varepsilon_{vv}$, and the solvation entropy Δs

$$G_{solv} = \Delta\varepsilon_{uv} + \Delta\varepsilon_{vv} - T\Delta s \tag{5}$$

The solvation entropy is given by the temperature derivative of the excess chemical potential at constant solvent density

$$\Delta s = -\left(\frac{\partial G_{solv}}{\partial T} \right)_\rho \tag{6}$$

The solute–solvent interaction energy and the solvent reorganization energy are respectively, defined by

$$\Delta\varepsilon_{uv} = E_{dist} + 4\pi \sum_\nu \rho_\nu \sum_{\alpha\gamma} \int r^2 u_{\alpha\gamma}(r) g_{\alpha\gamma}(r) \, dr \tag{7}$$

and

$$\Delta\varepsilon_{vv} = 2\pi \sum_\nu \rho_\nu^2 \sum_{\gamma\gamma'} \int r^2 u_{\gamma\gamma'}(r) \delta g_{\gamma\gamma'}(r) \, dr \tag{8}$$

The latter is the energy arising from the structural changes induced in the solvent. $\delta g_{\gamma\gamma'}$ is the first-order perturbation to $g_{\gamma\gamma'}$ created by inserting the solute molecule at infinite dilution.[37−39] In this study, we have calculated the solvent reorganization energy from the decomposition $\Delta\varepsilon_{vv} = \Delta\mu - (\Delta\varepsilon_{uv} - T\Delta s)$ instead of eq 8.

The RISM-SCF method has been implemented into the GAMESS program package for the electronic structure calculations.[40] The M06-2X/6-31G(d) were chosen as the density functional and basis set.[41] Assessment of the density functional in evaluating the TS structure of Diels–Alder reactions was reported by Linder and Brinck, and their results suggest to us that the M06-2X is a better choice than the other major functionals, such as BLYP, B3LYP, or PW91.[42] The RISM-SCF calculations were carried out at 298.15 K and the solvent density of 0.03334 molecule 10^3 nm^{-3} (= 0.9974 g cm^{-3}) using 2048 grids with width 0.05 Å. For the potential parameters of CP and MVK, the OPLSAA LJ parameters were employed.[43] For the solvent water molecules, we employed the SPC/E parameters for O and added the hydrogen LJ parameters to perform the RISM calculations because the original SPC/E model has no hydrogen LJ parameters.[44] We fixed the geometry of the solvent water molecules with an O–H distance of 1.0 Å and a H–O–H angle of 109.27°. The 1.0 and 5.0 M LiCl aqueous solutions were also prepared as a solvent system. The density and potential parameters of water and the temperature were the same as those for the ambient water mentioned above. The parameters of Li^+ and Cl^- ions

dx.doi.org/10.1021/jp4091552 | J. Phys. Chem. B 2013, 117, 14115−14121

were also chosen from the OPLSAA parameter set.[45] The values of the parameter sets for the solvents are summarized in Table 1. We employed the dielectric-consistent RISM

Table 1. Lennard-Jones Potential Parameters and Charges for Atom Sites of Solvent Used in RISM-SCF Calculations[a]

atom	σ (10^{-1} nm)	ε (kcal mol^{-1})	q (e)
O (water)	3.166	0.1554	−0.8476
H (water)	1.000	0.0545	0.4238
Li^+	2.126	0.0183	1.0000
Cl^-	4.417	0.1180	−1.0000

[a]The parameter set for water was taken from SPC/E[43] with modification on the H parameter and the set for ions from OPLSAA.[44].

(DRISM) method[46] to evaluate solvent−solvent systems with dielectric constants of 78.5, 64.2, and 33.3 for the water and 1.0 and 5.0 M LiCl aqueous solutions, respectively.[47] The DRISM method allows us to evaluate qualitatively reasonable site−site distribution functions for electrolytes in molecular solvents. We do not need to specify the effective point charges on the solute site as potential parameters because the effective charges can be generated from the RISM-SCF calculations. Molecular geometries of CP, MVK, *exo*-product, *endo*-product, and the TSs were calculated by means of the analytical energy gradients.[34] Vibrational frequencies were calculated at the same levels to evaluate Gibbs energies. The imaginary frequencies at the TSs were excluded in the calculations of the vibrational energy.

RESULTS AND DISCUSSION

TS Structures and Energetics. In a TS search, we found four TS structures, as *endo*-cis, *endo*-trans, *exo*-cis, and *exo*-trans, which are shown in Figure 1a−d, respectively. In the figure, the values of the distances between the two carbons that make chemical bond by the reaction are shown. The values in Figure 1 are for water, 1 M $LiCl_{aq}$, and 5 M $LiCl_{aq}$. With the increasing salt concentration, the distances between C4 and C12 increase slightly, while those between C3 and C13 decrease. The salt effects on the TS structures are quite small.

Table 2 summarizes the activation Gibbs energy of the reaction in water and $LiCl_{aq}$. The *endo*-trans TS structure shows the lowest activation energy in water. This result corresponds to the results of previous theoretical calculations.[2−5] Although the trend of stereoselectively is completely the same as that in $LiCl_{aq}$, the activation barriers became lower than those in water.

Figure 2 shows the Gibbs energy profiles of the reaction through the *endo*-trans TS. The changes in activation barrier of the *endo*-trans TS are 0.6 and 3.8 kcal mol^{-1} for 1 and 5 M $LiCl_{aq}$, respectively. These values are comparable with the experimental observation.[1]

In Table 3, the components of the Gibbs energy change from reactant states to each transition and product state are summarized. For all TSs, the changes of the solute electronic energy (ΔE_0) and kinetic free energy (ΔG_{kin}) are dominant, and those values are positive, while the solvation free energy (ΔG_{solv}) is minor and negative. The positive ΔG_{kin} can be attributed to the entropy loss from the C−C bond formation. In the product states, ΔE_0 becomes strongly negative because of the formation of the C−C bond, and ΔG_{kin} increases slightly with the progress of the reaction. Although ΔE_0 and ΔG_{kin} are dominant in determining the reaction profiles, they both have only weak dependency on the solvents. On the other hand,

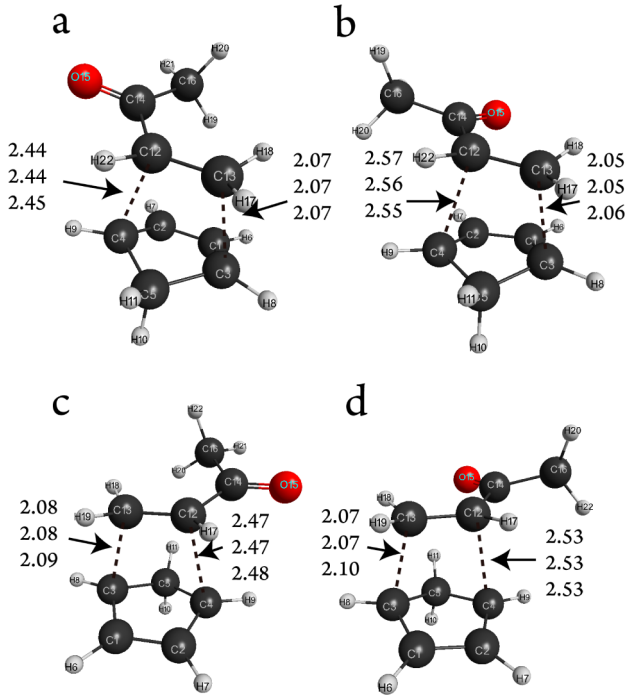

Figure 1. TS structures of (a) *endo*-cis, (b) *endo*-trans, (c) *exo*-cis, and (d) *exo*-trans. Values in the figure denote the distance between two atoms in 10^{-1} nm in water, 1 M $LiCl_{aq}$, and 5 M $LiCl_{aq}$, from top to bottom, respectively.

Table 2. Gibbs Energy[a] Changes in Water and 1 M and 5 M $LiCl_{aq}$

state	water	1 M $LiCl_{aq}$	5 M $LiCl_{aq}$
CP + MVK	0.0	0.0	0.0
TS/*endo*-cis	24.2	23.4	19.6
endo-trans	21.6	21.0	17.8
exo-cis	26.4	25.3	21.8
exo-trans	22.8	22.2	19.1
prod/*endo*	−13.3	−14.0	−17.5
exo	−13.4	−14.0	−16.7

[a]The unit of the Gibbs energies is given in kcal mol^{-1}.

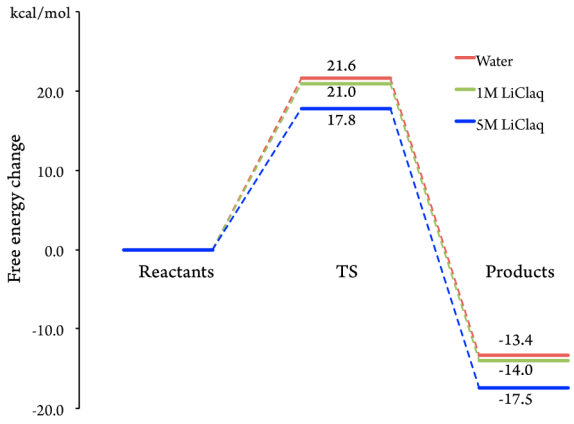

Figure 2. Gibbs energy profiles of the reaction through the *endo*-trans complex to the *endo*-products in water and 1 and 5 M $LiCl_{aq}$.

ΔG_{solv} shows strong dependency on the change of solvent components (see Table 4). In the next subsection, we discuss the solvent dependency of ΔG_{solv}.

dx.doi.org/10.1021/jp4091552 | J. Phys. Chem. B 2013, 117, 14115−14121

Table 3. Components of the Gibbs Energy[a] Change from Reactant States (CP + MVK)

state	solvent	ΔG	ΔE_0	ΔG_{kin}	ΔG_{solv}
CP + MVK	water	0.0	0.0	0.0	0.0
	1 M $LiCl_{aq}$	0.0	0.0	0.0	0.0
	5 M $LiCl_{aq}$	0.0	0.0	0.0	0.0
TS/	water	24.2	11.8	15.6	−3.1
endo-cis	1 M $LiCl_{aq}$	23.4	12.0	15.5	−4.0
	5 M $LiCl_{aq}$	19.6	12.6	15.4	−8.4
endo-trans	water	21.6	8.6	15.0	−1.9
	1 M $LiCl_{aq}$	21.0	8.5	15.0	−2.6
	5 M $LiCl_{aq}$	17.8	8.9	15.2	−6.2
exo-cis	water	26.4	13.5	14.9	−1.9
	1 M $LiCl_{aq}$	25.3	13.7	14.9	−3.4
	5 M $LiCl_{aq}$	21.8	14.1	14.9	−7.2
exo-trans	water	22.8	9.4	14.9	−1.5
	1 M $LiCl_{aq}$	22.2	9.4	14.9	−2.1
	5 M $LiCl_{aq}$	19.1	9.5	15.1	−5.6
prod/*endo*	water	−13.3	−33.5	18.3	1.8
	1 M $LiCl_{aq}$	−14.0	−33.5	18.3	1.2
	5 M $LiCl_{aq}$	−17.5	−33.4	18.5	−2.6
exo	water	−13.4	−34.1	18.3	2.4
	1 M $LiCl_{aq}$	−14.0	−34.1	18.3	1.8
	5 M $LiCl_{aq}$	−16.7	−34.1	19.2	−1.7

[a]The unit of the Gibbs energies is given in kcal mol^{-1}.

Table 4. Gibbs Energy[a] Changes from a Solution in Water to a Solution in $LiCl_{aq}$

	1 M $LiCl_{aq}$				5 M $LiCl_{aq}$			
state	δG	δE_0	δG_{kin}	δG_{solv}	δG	δE_0	δG_{kin}	δG_{solv}
CP	3.0	0.0	0.0	3.0	19.9	0.0	0.1	19.8
MVK	3.0	0.0	0.0	3.0	19.7	0.2	0.0	19.6
TS/*endo*-cis	5.2	0.2	−0.1	5.0	35.0	1.0	−0.2	34.1
endo-trans	5.4	0.0	0.1	5.3	35.8	0.5	0.2	35.1
exo-cis	4.8	0.2	0.0	4.6	35.0	0.8	0.1	34.2
exo-trans	5.4	0.0	0.0	5.4	35.9	0.3	0.2	35.4
prod/*endo*	5.3	0.0	0.0	5.3	35.5	0.3	0.2	35.0
exo	5.4	0.0	0.0	5.3	36.3	0.2	0.9	35.2

[a]The unit of the Gibbs energies is given in kcal mol^{-1}.

Salt Effects on the Reaction. The Gibbs energy changes of all molecules from water to $LiCl_{aq}$ and their components are listed in Table 4. Here, δ means the energy change corresponding to the change of solvents. At a glance, the total Gibbs energy changes of all species were positive, which means that $LiCl_{aq}$ makes all solute species unstable. For all molecules, the change of the solvation free energy, δG_{solv}, is dominant in the total Gibbs energy change, δG. Because the molecular structure changes caused by the changes in the solvent are relatively small, as can be seen in Figure 1, the kinetic energy changes are small. In the reactant, the sum of the total free-energy changes, 6.0 kcal mol^{-1} (1 M $LiCl_{aq}$) and 39.4 kcal mol^{-1} (5 M $LiCl_{aq}$), is larger than those in the TSs and product states. Therefore, it is conceivable that the major factor decreasing the activation barrier and/or increasing the rate of reaction is destabilization of the reactant species.

To clarify the reasons for this destabilization, we decomposed the solvation free energy by using eqs 5−8. In Table 5, the changes in the solvation free-energy components from the water to $LiCl_{aq}$ are summarized. The major factors causing destabilization of all species are the solvation entropy and the solvent reorganization. It is indicated that the hydrophobic effects between solute and solvent are increased by adding LiCl. The hydrophobic effects strongly depend on the solvent-accessible surface area,[39] which is reduced by the C−C bond formation between CP and MVK. Therefore, $\delta(-T\Delta s)$ decreases with the progress of the reaction. On the other hand, the solute−solvent interaction energy changes $\delta\Delta\varepsilon_{uv}$ associated with the addition of LiCl are small. Nevertheless, they are important in determining the reaction rate. The changes of $\delta\Delta\varepsilon_{uv}$ from the reactant state are larger than those of $\delta(-T\Delta s)$ (see parentheses in Table 5). It is indicated that the C−C bond formation stablilizes the interaction between solute and solvent.

Solvation Structure. To consider the reason for the stabilization of the solute−solvent interaction associated with the LiCl addition, the distributions of solvent species around solute molecules were examined using RDFs. Because the *endo*-trans TS structure is the most stable among the TS structures as elucidated by the analysis of the Gibbs energy changes, we focus our discussion on that structure.

In Figure 3, the RDFs between solvent water and the carbonyl oxygen of the stable MVK and TS structures are depicted. While the two distributions of oxygen show small differences between the stable MVK and TS structures (Figure 3a), those of hydrogen show conspicuous change on the first peak (Figure 3b). The height of the first peak in the RDFs of hydrogen directly signifies the degree of hydrogen bonding. It indicates that the strength of the hydrogen bond is enhanced in the process of reaction. As a result, the TS is stabilized by the hydrogen bond compared with the reactant state. The difference in the solute−solvent RDFs between the reactant

Table 5. Change of Solvation Free Energy Components from Water to $LiCl_{aq}$[a]

	1 M $LiCl_{aq}$				5 M $LiCl_{aq}$			
state	δG_{solv}	$\delta(-T\Delta s)$	$\delta\Delta\varepsilon_{uv}$	$\delta\Delta\varepsilon_{vv}$	δG_{solv}	$\delta(-T\Delta s)$	$\delta\Delta\varepsilon_{uv}$	$\delta\Delta\varepsilon_{vv}$
CP	3.0	1.8	0.2	1.1	19.8	9.9	1.8	8.1
MVK	3.0	1.8	−0.2	1.3	19.6	10.2	−0.2	9.6
TS/*endo*-cis	5.0(−1.0)	3.4(−0.2)	−0.9(−0.9)	2.5(0.1)	34.1(−5.3)	18.7(−1.4)	−2.4(−4.0)	17.8 (0.1)
endo-trans	5.3(−0.7)	3.4(−0.2)	−0.3(−0.3)	2.3(−0.1)	35.1(−4.3)	18.6(−1.5)	−0.4(−2.0)	16.9(−0.8)
exo-cis	4.6(−1.4)	3.5(−0.1)	−2.2(−2.2)	3.2(0.8)	34.2(−5.2)	18.9(−1.2)	−3.2(−4.8)	18.4(0.7)
exo-trans	5.4(−0.6)	3.4(−0.2)	−0.3(−0.3)	2.3(−0.1)	35.4(−4.0)	18.8(−1.3)	−0.3(−1.9)	16.9(−0.8)
prod/*endo*	5.3(−0.7)	3.3(−0.3)	0.0(0.0)	2.1(−0.3)	35.0(−4.4)	18.4(−1.7)	0.8(−0.8)	15.8(−1.9)
exo	5.3(−0.7)	3.3(−0.3)	0.0(0.0)	2.0(−0.4)	35.2(−4.2)	18.4(−1.7)	1.3(−0.3)	15.6(−2.1)

[a]Numbers in parentheses denote the changes from the reactant states. The unit of the Gibbs energies is given in kcal mol^{-1}.

dx.doi.org/10.1021/jp4091552 | J. Phys. Chem. B 2013, 117, 14115−14121

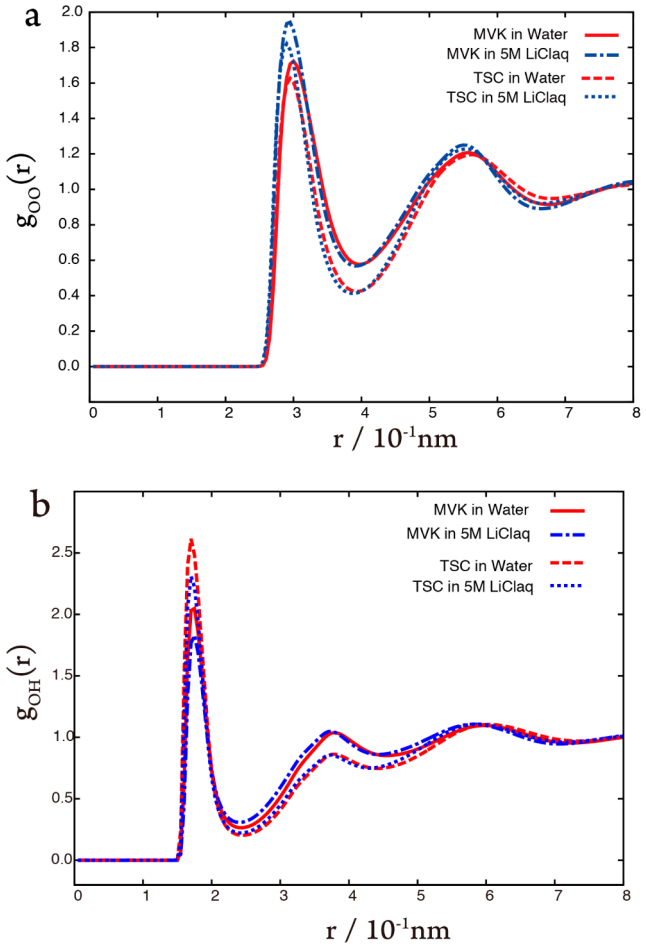

Figure 3. RDF of water oxygen (a) and hydrogen (b) around the carbonyl oxygen of MVK and the TS *endo*-trans complex (TSC) in water and 5 M $LiCl_{aq}$.

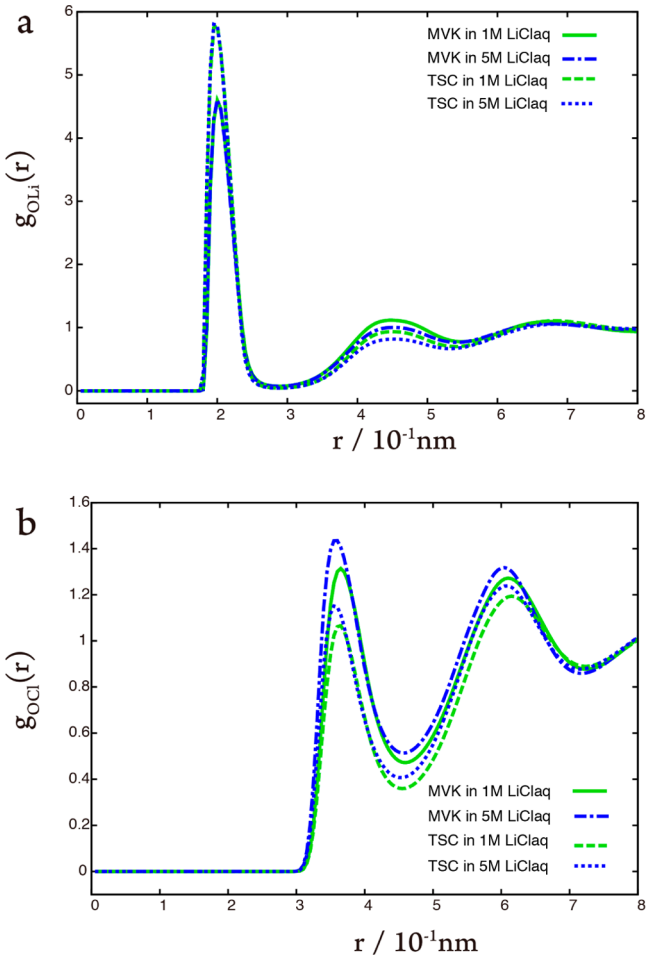

Figure 4. RDF of Li^+ (a) and Cl^- (b) around the carbonyl oxygen of MVK and the TS *endo*-trans complex (TSC) in 1 and 5 M $LiCl_{aq}$.

and TSs does not change much when the salt is added to the solution.

In Figure 4, the RDFs between the ions and the solute molecule are compared. The distribution of Li^+ and Cl^- around the carbonyl oxygen shows the behavior similar to the hydrogen and oxygen of water, respectively, because they have the same signs of effective charge. Therefore, the effects on the solute molecule are also similar to those of hydrogen and oxygen of the solvent water. As mentioned above, the interaction between Li^+ and the carbonyl oxygen can stabilize the solute molecule (see Figure 4a). On the other hand, the first peak of Cl^- decreases as the reaction progresses (see Figure 4b). Because both the Cl^- and the carbonyl oxygen have negative effective charges, the interaction between Cl^- and the carbonyl oxygen is repulsive; thus, decreasing the interaction makes the TS structure stable. These two interactions cooperatively affect the decrease in the activation barrier of the reaction.

CONCLUSIONS

The salt effects on the Diels–Alder reaction of CP with MVK have been investigated by means of the RISM-SCF theory. The rate of the reaction is accelerated by adding LiCl to the water solvent in harmony with the corresponding experiments. This behavior is attributed to increased hydrophobic effects between solute and solvent. The four *endo*/*exo* and cis/trans TS structures were found by geometry optimization of the CP and MVK complexes. The *endo*-trans structure showed the lowest energy in both water and LiCl aqueous solutions. The activation barrier calculations show good agreement with the experiments. The activation barriers of the reaction in 1 and 5 M LiCl solutions were 0.6 and 3.8 kcal mol^{-1} lower than that in water, respectively. The analyses of the Gibbs energy changes and solvation structures elucidated the mechanism of the salt effects on the reaction. Although the total Gibbs energy changes of all of the species are positive, the sum of the total Gibbs energy changes of reactant species is larger than those of the TSs. The salt effect of LiCl makes all species in the reaction unstable by the hydrophobic effect; however, the increase of hydrophobic effect in the TS complexes is suppressed by making the hydrogen bond, which is stronger compared with the reactant MVK.

AUTHOR INFORMATION

Corresponding Authors

*E-mail: noriwo@chem.kyushu-univ.jp. Phone: +81(Japan)-92-642-2588 (N.Y.).

*E-mail: hirataf@fc.ritsumei.ac.jp. Phone: +81-77-561-2617 (F.H.).

Author Contributions

The manuscript was written with contributions from all authors. All authors have given approval to the final version of the manuscript.

dx.doi.org/10.1021/jp4091552 | *J. Phys. Chem. B* 2013, 117, 14115–14121

Funding

We would like to thank the Next Generation Supercomputing Project, Nanoscience Program and the Strategic Programs for Innovative Research (SPIRE) and the Computational Materials Science Initiative (CMSI), Japan for their support. N.Y. is grateful for a Grant-in-Aid (22740279, 25410021) from MEXT, Japan and to the Sumitomo Foundation.

Notes

The authors declare no competing financial interest.

■ ACKNOWLEDGMENTS

The authors are grateful to Prof. H. Nakano at Kyushu University for invaluable discussions. Numerical calculations were partly carried out in the Research Center for Computational Science, Institute for Molecular Science, National Institutes of Natural Science.

■ ABBREVIATIONS

RISM, reference interaction site model; RISM-SCF, RISM self-consistent field; MVK, methyl vinyl ketone; CP, cyclopentadiene; TS, transition state; RDF, radial distribution function

■ REFERENCES

(1) Rideout, D.; Breslow, R. Hydrophobic Acceleration of Diels–Alder Reactions. *J. Am. Chem. Soc.* **1980**, *102*, 7816–7817.

(2) Jorgensen, W. L.; Lim, D. C.; Blake, J. F. Ab Initio Study of Diels–Alder Reactions of Cyclopentadiene with Ethylene, Isoprene, Cyclopentadiene, Acrylonitrile, and Methyl Vinyl Ketone. *J. Am. Chem. Soc.* **1993**, *115*, 2936–2942.

(3) Jorgensen, W. L.; Lim, D.; Blake, J. F. Solvent Effects on the Diels–Alder Reaction of Methyl Vinyl Ketone and Cyclopentadiene from Computer-Simulations. *NATO Adv. Sci. Inst. Ser.* **1993**, *398*, 377–387.

(4) Harano, Y.; Sato, H.; Hirata, F. A Theoretical Study on a Diels–Alder Reaction in Ambient and Supercritical Water: Viewing Solvent Effects Through Frontier Orbitals. *Chem. Phys.* **2000**, *258*, 151–161.

(5) Harano, Y.; Sato, H.; Hirata, F. Solvent Effects on a Diels–Alder Reaction in Supercritical Water: RISM-SCF Study. *J. Am. Chem. Soc.* **2000**, *122*, 2289–2293.

(6) Chandrasekhar, J.; Shariffskul, S.; Jorgensen, W. L. QM/MM Simulations for Diels–Alder Reactions in Water: Contribution of Enhanced Hydrogen Bonding at the Transition State to the Solvent Effect. *J. Phys. Chem. B* **2002**, *106*, 8078–8085.

(7) Corey, E. J. Catalytic Enantioselective Diels–Alder Reactions: Methods, Mechanistic Fundamentals, Pathways, and Applications. *Angew. Chem., Int. Ed.* **2002**, *41*, 1650–1667.

(8) Nicolaou, K. C.; Snyder, S. A.; Montagnon, T.; Vassilikogiannakis, G. The Diels–Alder Reaction in Total Synthesis. *Angew. Chem., Int. Ed.* **2002**, *41*, 1668–1698.

(9) DeChancie, J.; Acevedo, O.; Evanseck, J. D. Density Functional Theory Determination of an Axial Gateway to Explain the Rate and Endo Selectivity Enhancement of Diels–Alder Reactions by Bis-(oxazoline)-Cu(II). *J. Am. Chem. Soc.* **2004**, *126*, 6043–6047.

(10) Guimarães, C. R. W.; Udier-Blagoviæ, M.; Jorgensen, W. L. Macrophomate Synthase: QM/MM Simulations Address the Diels–Alder versus Michael–Aldol Reaction Mechanism. *J. Am. Chem. Soc.* **2005**, *127*, 3577–3588.

(11) Pieniazek, S. N.; Houk, K. N. The Origin of the Halogen Effect on Reactivity and Reversibility of Diels–Alder Cycloadditions Involving Furan. *Angew. Chem., Int. Ed.* **2006**, *45*, 1442–1445.

(12) Acevedo, O.; Jorgensen, W. L.; Evanseck, J. D. Elucidation of Rate Variations for a Diels–Alder Reaction in Ionic Liquids from QM/MM Simulations. *J. Chem. Theory Comput.* **2007**, *3*, 132–138.

(13) Hayaki, S.; Kido, K.; Yokogawa, D.; Sato, H.; Sakaki, S. A Theoretical Analysis of a Diels–Alder Reaction in Ionic Liquids. *J. Phys. Chem. B* **2009**, *113*, 8227–8230.

(14) Kong, S.; Evanseck, J. D. Density Functional Theory Study of Aqueous-Phase Rate Acceleration and Endo/Exo Selectivity of the Butadiene and Acrolein Diels–Alder Reaction. *J. Am. Chem. Soc.* **2000**, *122*, 10418–10427.

(15) Tomasi, J.; Mennucci, B.; Cammi, R. Quantum Mechanical Continuum Solvation Models. *Chem. Rev.* **2005**, *105*, 2999–3093.

(16) Frenkel, D.; Smit, B. *Understanding Molecular Simulation: From Algorithms to Applications*, 2nd ed.; Academic Press: San Diego, CA, 2001.

(17) Ten-no, S.; Hirata, F.; Kato, S. A Hybrid Approach for the Solvent Sffect on the Electronic Structure of a Solute Based on the RISM and Hartree–Fock Equations. *Chem. Phys. Lett.* **1993**, *214*, 391–396.

(18) Ten-No, S.; Hirata, F.; Kato, S. Reference Interaction Site Model Self-Consistent-Field Study for Solvation Effect on Carbonyl-Compounds in Aqueous-Solution. *J. Chem. Phys.* **1994**, *100*, 7443–7453.

(19) Chandler, D.; Andersen, H. Optimized Cluster Expansions for Classical Fluids. 2. Theory of Molecular Liquids. *J. Chem. Phys.* **1972**, *57*, 1930–1937.

(20) Hirata, F.; Rossky, P. An Extended RISM Equation for Molecular Polar Fluids. *Chem. Phys. Lett.* **1981**, *83*, 329–334.

(21) Zichi, D. A.; Rossky, P. J. Molecular Conformational Equilibria in Liquids. *J. Chem. Phys.* **1986**, *84*, 1712–1723.

(22) Hirata, F.; Pettitt, B. M.; Rossky, P. J. Application of an Extended RISM Equation to Dipolar and Quadrupolar Fluids. *J. Chem. Phys.* **1982**, *77*, 509–520.

(23) Hirata, F.; Rossky, P. J.; Montgomery Pettitt, B. The Interionic Potential of Mean Force in a Molecular Polar Solvent From an Extended RISM Equation. *J. Chem. Phys.* **1983**, *78*, 4133–4144.

(24) Hirata, F. *Molecular Theory of Solvation*; Kluwer: Dordrecht, The Netherlands, 2003.

(25) Pettitt, B. M.; Rossky, P. J. The Contribution of Hydrogen Bonding to the Structure of Liquid Methanol. *J. Chem. Phys.* **1982**, *78*, 7296–7299.

(26) Pettitt, B.; Rossky, P. Integral Equation Predictions of Liquid State Structure for Waterlike Intermolecular Potentials. *J. Chem. Phys.* **1982**, *77*, 1451–1457.

(27) Sato, H.; Hirata, F. Ab Initio Study of Water. II. Liquid Structure, Electronic and Thermodynamic Properties over a Wide Range of Temperature and Density. *J. Chem. Phys.* **1999**, *111*, 8545–8555.

(28) Yoshida, N.; Imai, T.; Phongphanphanee, S.; Kovalenko, A.; Hirata, F. Molecular Recognition in Biomolecules Studied by Statistical-Mechanical Integral-Equation Theory of Liquids. *J. Phys. Chem. B* **2009**, *113*, 873–886.

(29) Yokogawa, D.; Sato, H.; Sakaki, S. New Generation of the Reference Interaction Site Model Self-Consistent Field Method: Introduction Of Spatial Electron Density Distribution to the Solvation Theory. *J. Chem. Phys.* **2007**, *126*, 244504.

(30) Imai, T.; Kinoshita, M.; Hirata, F. Salt Effect on Stability and Solvation Structure of Peptide: An Integral Equation Study. *Bull. Chem. Soc. Jpn.* **2000**, *73*, 1113–1122.

(31) Yoshida, N.; Phongphanphanee, S.; Maruyama, Y.; Imai, T.; Hirata, F. Selective Ion-Binding by Protein Probed with the 3D-RISM Theory. *J. Am. Chem. Soc.* **2006**, *128*, 12042–12043.

(32) Yoshida, N.; Phongphanphanee, S.; Hirata, F. Selective Ion Binding by Human Lysozyme Studied by the Statistical Mechanical Integral Equation Theory. *Lect. Ser. Comput. Comput. Sci.* **2006**, *6*, 1–3.

(33) Yoshida, N.; Phongphanphanee, S.; Hirata, F. Selective Ion Binding by Protein Probed with the Statistical Mechanical Integral Equation Theory. *J. Phys. Chem. B* **2007**, *111*, 4588–4595.

(34) Sato, H.; Hirata, F.; Kato, S. Analytical Energy Gradient for the Reference Interaction Site Model Multiconfigurational Self-Consistent-Field Method: Application to 1,2-Difluoroethylene in Aqueous Solution. *J. Chem. Phys.* **1996**, *105*, 1546–1551.

(35) Kovalenko, A.; Hirata, F. Potential of Mean Force between Two Molecular Ions in a Polar Molecular Solvent: A Study by the Three-Dimensional Reference Interaction Site Model. *J. Phys. Chem. B* **1999**, *103*, 7942−7957.
(36) Kovalenko, A.; Hirata, F. Potentials of Mean Force of Simple Ions in Ambient Aqueous Solution. I. Three-Dimensional Reference Interaction Site Model Approach. *J. Chem. Phys.* **2000**, *112*, 10391−10402.
(37) Yu, H. A.; Karplus, M. A Thermodynamic Analysis of Solvation. *J. Chem. Phys.* **1988**, *89*, 2366−2379.
(38) Yu, H. A.; Roux, B.; Karplus, M. Solvation Thermodynamics: An Approach from Analytic Temperature Derivatives. *J. Chem. Phys.* **1990**, *92*, 5020.
(39) Imai, T.; Harano, Y.; Kinoshita, M.; Kovalenko, A.; Hirata, F. A Theoretical Analysis on Hydration Thermodynamics of Proteins. *J. Chem. Phys.* **2006**, *125*, 024911.
(40) Schmidt, M. W.; Baldridge, K. K.; Boatz, J. A.; Elbert, S. T.; Gordon, M. S.; Jensen, J. H.; Koseki, S.; Matsunaga, N.; Nguyen, K. A.; Su, S.; Windus, T. L.; Dupuis, M.; Montgomery, J. A. General Atomic and Molecular Electronic Structure System. *J. Comput. Chem.* **1993**, *14*, 1347−1363.
(41) Zhao, Y.; Truhlar, D. G. The M06 Suite of Density Functionals for Main Group Thermochemistry, Thermochemical Kinetics, Noncovalent Interactions, Excited States, and Transition Elements: Two New Functionals and Systematic Testing of Four M06-class Functionals and 12 Other Functionals. *Theor. Chem. Acc.* **2008**, *120*, 215−241.
(42) Linder, M.; Brinck, T. On the Method-Dependence of Transition State Asynchronicity in Diels−Alder Reactions. *Phys. Chem. Chem. Phys.* **2013**, *15*, 5108−5114.
(43) Chandrasekhar, J.; Spellmeyer, D. C.; Jorgensen, W. L. Energy Component Analysis for Dilute Aqueous-Solutions of Li^+, Na^+, F^-, and Cl^- Ions. *J. Am. Chem. Soc.* **1984**, *106*, 903−910.
(44) Berendsen, H. J. C.; Grigera, J. R.; Straatsma, T. P. The Missing Term in Effective Pair Potentials. *J. Phys. Chem.* **1987**, *91*, 6269−6271.
(45) Aqvist, J. Ion Water Interaction Potentials Derived from Free-Energy Perturbation Simulations. *J. Phys. Chem.* **1990**, *94*, 8021−8024.
(46) Perkyns, J. S.; Pettitt, B. M. A Dielectrically Consistent Interaction Site Theory for Solvent Electrolyte Mixtures. *Chem. Phys. Lett.* **1992**, *190*, 626−630.
(47) Wei, Y.-Z.; Sridhar, S. Dielectric Spectroscopy Up to 20 GHz of LiCl/H_2O Solutions. *J. Chem. Phys.* **1990**, *92*, 923.